

# Gradient Based Methods for Non-Smooth Regularization Via Convolution Smoothing

Sergey Voronin<sup>1</sup> and Davis Yoshida<sup>1</sup>

<sup>1</sup>Department of Applied Mathematics, University of Colorado, Boulder, CO 80309, USA

March 28, 2022

## Abstract

We present a smoothing technique which allows for the use of gradient based methods (such as steepest descent and conjugate gradients) for non-smooth regularization of inverse problems. As an application of this technique, we consider the problem of finding regularized solutions of linear systems  $Ax = b$  with sparsity constraints. Such problems involve the minimization of a functional with an absolute value term, which is not smooth. We replace the non-smooth term by a smooth approximation, computed via a convolution. We are then able to compute gradients and Hessians, and utilize standard gradient based methods which yield good numerical performance in few iterations.

## 1 Introduction

Consider the linear system  $Ax = b$ , where  $A \in \mathbb{R}^{m \times n}$  and  $b \in \mathbb{R}^m$ . We assume no specific relation between  $m$  and  $n$ , although often, in linear systems arising from physical inverse problems, we have more unknowns than data:  $m \ll n$  [18]. In such a setting, it is common to introduce a constraint on the solution, both to account for the possible ill-conditioning in  $A$  and noise in  $b$  (regularization) and for the lack of data with respect to the number of unknown variables in the linear system. A commonly used constraint is sparsity: to require the solution  $x$  to have few nonzero elements compared to the dimension of  $x$ . A common way of finding a sparse solution to the under-determined linear system  $Ax = b$  is to solve the classical Lasso problem [8]. That is, find  $\bar{x} = \arg \min_x F_1(x)$  where

$$F_1(x) = \|Ax - b\|_2^2 + 2\tau \|x\|_1,$$

i.e., the least squares problem with an  $\ell_1$  regularizer, governed by the parameter  $\tau > 0$  [6]. For any  $p \geq 1$ , the map  $\|x\|_p := (\sum_{k=1}^n |x_k|^p)^{\frac{1}{p}}$  (for any  $x \in \mathbb{R}^n$ ) is called the  $\ell_p$ -norm on  $\mathbb{R}^n$ . For  $p = 1$ , the  $\|\cdot\|_1$  norm is called an  $\ell_1$  norm and is convex. Besides  $F_1(x)$ , we also consider the more general  $\ell_p$  functional:

$$F_p(x) = \|Ax - b\|_2^2 + 2\tau \left( \sum_{k=1}^n |x_k|^p \right)^{\frac{1}{p}}, \quad (1.1)$$

where  $p > 0$  is not necessarily above 1. As  $p \rightarrow 0$ , the right term of this functional approximates the count of nonzeros or the so called  $\ell_0$  “norm” (which is not a proper norm):

$$\|x\|_0 = \lim_{p \rightarrow 0} \|x\|_p = \lim_{p \rightarrow 0} \left( \sum_{k=1}^n |x_k|^p \right)^{1/p},$$

which can be seen from Figure 1.

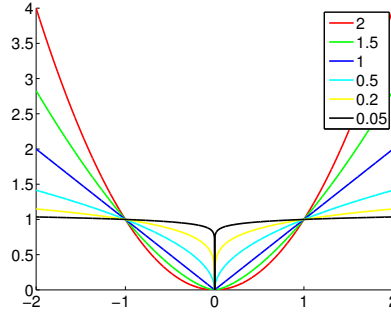


Figure 1:  $|x|^p$  plotted for different values of  $p$ , as  $p \rightarrow 0$ , the plot approaches an indicator function.

For  $0 < p < 1$ , (1.1) is not convex. However, the minimization of non-smooth non-convex functions has been shown to produce good results in some compressive sensing applications [3]. The non-smoothness of the functional  $F_p(x)$ , however, complicates its minimization from an algorithmic point of view. The non-smooth part of (1.1) is due to the absolute value function  $g(x_k) = |x_k|$ . Because the gradient of  $F_p(x)$  cannot be obtained, different minimization techniques such as sub-gradient methods are usually used [16]. For the convex  $p = 1$  case, various thresholding based methods have become popular. A particularly successful example is the soft thresholding based method FISTA [2]. This algorithm is based on the acceleration of a soft thresholded Landweber iteration:

$$x^{k+1} = \mathbb{S}_\tau(x^k + A^T b - A^T A x^k),$$

which is known to converge, but slowly, to the  $\ell_1$  minimizer [6]. The soft thresholding function  $\mathbb{S}_\tau : \mathbb{R}^n \rightarrow \mathbb{R}^n$  is defined by

$$(\mathbb{S}_\tau(x))_k = \text{sgn}(x_k) \max\{0, |x_k| - \tau\}, \quad \forall k = 1, \dots, n, \quad \forall x \in \mathbb{R}^n.$$

The thresholding is performed on  $x^k - \nabla_x(\frac{1}{2}\|Ax^k - b\|_2^2) = x^k - A^T(Ax^k - b)$ , which is a very simple gradient based scheme with a constant line search [9]. Naturally, more advanced gradient schemes may be able to provide better numerical performance; however, they are possible to utilize only if we are able to compute the gradient of the functional we want to minimize.

In our approach, we use an approximation to the non-smooth absolute value function (which appears in functionals like  $F_p(x)$  for sparsity constrained regularization) via a convolution with a Gaussian function. This allows us to replace the non-smooth objective function  $F_p(x)$  by a smooth functional  $H_{p,\sigma}(x)$ , which is close to  $F_p(x)$  in value (as the parameter  $\sigma \rightarrow 0$ ). Since the approximating functional  $H_{p,\sigma}(x)$  is smooth, we can compute its gradient  $\nabla_x H_{p,\sigma}(x)$ . We are then able to use gradient

based algorithms such as steepest descent and conjugate gradients to approximately minimize  $F_p(x)$  by working with the approximate functional and gradient pair. The resulting gradient based methods we show are simple to implement and yield good numerical performance.

We remark that this article is not the first in attempting to use smooth approximations for sparsity constrained problems. A smooth  $\ell_0$  norm approach has been proposed in [11]. In this article, we propose a more general method which can be used for  $F_p(x)$ , including the popular  $\ell_1$  case. Sparsity constrained regularization is just one application of the convolution based smoothing approach we introduce here and we believe that the same idea can be used in different applications.

## 2 Mollifiers and Approximation via Convolution

In mathematical analysis, the concept of mollifiers is well known. Below, we state the definition and convergence result regarding mollifiers, as exhibited in [7]. A smooth function  $\psi_\sigma : \mathbb{R} \rightarrow \mathbb{R}$  is said to be a (non-negative) *mollifier* if it has finite support, is non-negative ( $\psi \geq 0$ ), and has area  $\int_{\mathbb{R}} \psi(t) dt = 1$ . For any mollifier  $\psi$  and any  $\sigma > 0$ , define the parametric function  $\psi_\sigma : \mathbb{R} \rightarrow \mathbb{R}$  by:  $\psi_\sigma(t) := \frac{1}{\sigma} \psi\left(\frac{t}{\sigma}\right)$ , for all  $t \in \mathbb{R}$ . Then  $\{\psi_\sigma : \sigma > 0\}$  is a family of mollifiers, whose support decreases as  $\sigma \rightarrow 0$ , but the volume under the graph always remains equal to one. We then have the following important lemma for the approximation of functions, whose proof is given in [7].

**Lemma 2.1** *For any continuous function  $g \in L^1(\Theta)$  with compact support and  $\Theta \subseteq \mathbb{R}$ , and any mollifier  $\psi : \mathbb{R} \rightarrow \mathbb{R}$ , the convolution  $\psi_\sigma * g$ , which is the function defined by:*

$$(\psi_\sigma * g)(t) := \int_{\mathbb{R}} \psi_\sigma(t-s)g(s)ds = \int_{\mathbb{R}} \psi_\sigma(s)g(t-s)ds, \quad \forall t \in \mathbb{R},$$

*converges uniformly to  $g$  on  $\Theta$ , as  $\sigma \rightarrow 0$ .*

Inspired by the above results, we will now use convolution with approximate mollifiers to approximate the absolute value function  $g(t) = |t|$  (which is not in  $L^1(\mathbb{R})$ ) with a smooth function. We start with the Gaussian function  $K(t) = \frac{1}{\sqrt{2\pi}} \exp\left(-\frac{t^2}{2}\right)$  (for all  $t \in \mathbb{R}$ ), and introduce the  $\sigma$ -dependent family:

$$K_\sigma(t) := \frac{1}{\sigma} K\left(\frac{t}{\sigma}\right) = \frac{1}{\sqrt{2\pi\sigma^2}} \exp\left(-\frac{t^2}{2\sigma^2}\right), \quad \forall t \in \mathbb{R}. \quad (2.1)$$

This function is not a mollifier because it does not have finite support. However, this function is coercive, that is, for any  $\sigma > 0$ ,  $K_\sigma(t) \rightarrow 0$  as  $|t| \rightarrow \infty$ . In addition, we have that  $\int_{-\infty}^{\infty} K_\sigma(t) dt = 1$  for all  $\sigma > 0$ :

$$\begin{aligned} \int_{-\infty}^{\infty} K_\sigma(t) dt &= \frac{1}{\sqrt{2\pi\sigma^2}} \int_{\mathbb{R}} \exp\left(-\frac{t^2}{2\sigma^2}\right) dt = \frac{2}{\sqrt{2\pi\sigma^2}} \int_0^{\infty} \exp\left(-\frac{t^2}{2\sigma^2}\right) dt \\ &= \frac{2}{\sqrt{2\pi\sigma^2}} \int_0^{\infty} \exp(-u^2) \sqrt{2}\sigma du = \frac{2}{\sqrt{2\pi\sigma^2}} \sqrt{2}\sigma \frac{\sqrt{\pi}}{2} = 1. \end{aligned}$$

Figure 2 below presents a plot of the function  $K_\sigma$  in relation to the parameter  $\sigma$ . We see that  $K_\sigma(t) \geq 0$  and  $K_\sigma(t)$  is very close to zero for  $|t| > 4\sigma$ . In this sense, the function  $K_\sigma$  is an approximate mollifier.

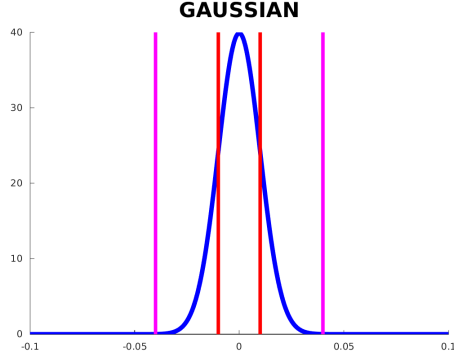


Figure 2:  $K_\sigma(t)$  and vertical lines at  $(-\sigma, \sigma)$  and  $(-4\sigma, 4\sigma)$  for  $\sigma = 0.01$ .

Let us now compute the limit  $\lim_{\sigma \rightarrow 0} K_\sigma(t)$ . For  $t = 0$ , it is immediate that  $\lim_{\sigma \rightarrow 0} K_\sigma(0) = \infty$ . For  $t \neq 0$ , we use l'Hôspital's rule:

$$\lim_{\sigma \rightarrow 0} K_\sigma(t) = \lim_{\sigma \rightarrow 0} \frac{1}{\sqrt{2\pi\sigma^2}} \exp\left(-\frac{t^2}{2\sigma^2}\right) = \lim_{\gamma \rightarrow \infty} \frac{\gamma}{\sqrt{2\pi} \exp\left(\frac{\gamma^2 t^2}{2}\right)} = \frac{1}{\sqrt{2\pi}} \lim_{\gamma \rightarrow \infty} \frac{1}{\gamma t^2 \exp\left(\frac{\gamma^2 t^2}{2}\right)} = 0,$$

with  $\gamma = \frac{1}{\sigma}$ . We see that  $K_\sigma(t)$  behaves like a Dirac delta function  $\delta_0(x)$  with unit integral over  $\mathbb{R}$  and the same pointwise limit. Thus, for small  $\sigma > 0$ , we expect that the absolute value function can be approximated by its convolution with  $K_\sigma$ , i.e.,

$$|t| \approx \phi_\sigma(t), \quad \forall t \in \mathbb{R}, \quad (2.2)$$

where the function  $\phi_\sigma : \mathbb{R} \rightarrow \mathbb{R}$  is defined as the convolution of  $K_\sigma$  with the absolute value function:

$$\phi_\sigma(t) := (K_\sigma * |\cdot|)(t) = \frac{1}{\sqrt{2\pi\sigma^2}} \int_{-\infty}^{\infty} |t-s| \exp\left(-\frac{s^2}{2\sigma^2}\right) ds, \quad \forall t \in \mathbb{R}. \quad (2.3)$$

We show in Proposition 2.4 below, that the approximation in (2.2) converges in the  $L^1$  norm (as  $\sigma \rightarrow 0$ ). The advantage of using this approximation is that  $\phi_\sigma$ , unlike the absolute value function, is a smooth function.

Before we state the convergence result in Proposition 2.4, we express the convolution integral and its derivative in terms of the well-known error function [1].

**Lemma 2.2** *For any  $\sigma > 0$ , define  $\phi_\sigma : \mathbb{R} \rightarrow \mathbb{R}$  as in (2.3). Then we have that for all  $t \in \mathbb{R}$ :*

$$\phi_\sigma(t) = t \operatorname{erf}\left(\frac{t}{\sqrt{2}\sigma}\right) + \sqrt{\frac{2}{\pi}} \sigma \exp\left(-\frac{t^2}{2\sigma^2}\right), \quad (2.4)$$

$$\frac{d}{dt} \phi_\sigma(t) = \operatorname{erf}\left(\frac{t}{\sqrt{2}\sigma}\right), \quad (2.5)$$

where the error function is defined as:

$$\operatorname{erf}(t) = \frac{2}{\sqrt{\pi}} \int_0^t \exp(-u^2) du \quad \forall t \in \mathbb{R}.$$

**Proof.** Fix  $\sigma > 0$ . Define  $C_\sigma : \mathbb{R}_+ \times \mathbb{R}$  by

$$C_\sigma(T, t) := \int_{-T}^T |t - s| K_\sigma(s) ds = \frac{1}{\sqrt{2\pi\sigma^2}} \int_{-T}^T |t - s| \exp\left(-\frac{s^2}{2\sigma^2}\right) ds, \quad \forall t \in \mathbb{R}, T \geq 0.$$

We can remove the absolute value sign in the integration above by breaking up the integral into intervals from  $-T$  to  $t$  and from  $t$  to  $T$  where  $|t - s|$  can be replaced by  $(t - s)$  and  $(s - t)$ , respectively. Expanding the above we have that:

$$\begin{aligned} \sqrt{2\pi\sigma^2} C_\sigma(T, t) &= \int_{-T}^T |t - s| \exp\left(-\frac{s^2}{2\sigma^2}\right) ds \\ &= \int_{-T}^t (t - s) \exp\left(-\frac{s^2}{2\sigma^2}\right) ds + \int_t^T (s - t) \exp\left(-\frac{s^2}{2\sigma^2}\right) ds \\ &= t \left( \int_{-T}^t \exp\left(-\frac{s^2}{2\sigma^2}\right) ds - \int_t^T \exp\left(-\frac{s^2}{2\sigma^2}\right) ds \right) \\ &\quad + \int_{-T}^t \exp\left(-\frac{s^2}{2\sigma^2}\right) (-s) ds + \int_t^T \exp\left(-\frac{s^2}{2\sigma^2}\right) s ds \\ &= \sqrt{2}\sigma t \left( \int_{-T/\sqrt{2}\sigma}^{t/\sqrt{2}\sigma} \exp(-u^2) du - \int_{t/\sqrt{2}\sigma}^{T/\sqrt{2}\sigma} \exp(-u^2) du \right) \\ &\quad + \sigma^2 \left( \int_{-T}^t \exp\left(-\frac{s^2}{2\sigma^2}\right) \left(-\frac{s}{\sigma^2}\right) ds - \int_t^T \exp\left(-\frac{s^2}{2\sigma^2}\right) \left(-\frac{s}{\sigma^2}\right) ds \right). \end{aligned}$$

Next, making use of the definition of the error function, the fact that it's an odd function (i.e.  $\operatorname{erf}(-t) = -\operatorname{erf}(t)$ ), and of the fundamental theorem of calculus, we have:

$$\begin{aligned} \sqrt{2\pi\sigma^2} C_\sigma(T, t) &= \sqrt{\frac{\pi}{2}} \sigma t \left( \operatorname{erf}\left(\frac{t}{\sqrt{2}\sigma}\right) - \operatorname{erf}\left(\frac{-T}{\sqrt{2}\sigma}\right) - \operatorname{erf}\left(\frac{T}{\sqrt{2}\sigma}\right) + \operatorname{erf}\left(\frac{t}{\sqrt{2}\sigma}\right) \right) \\ &\quad + \sigma^2 \left( \int_{-T}^t \frac{d}{ds} \left( \exp\left(-\frac{s^2}{2\sigma^2}\right) \right) ds - \int_t^T \frac{d}{ds} \left( \exp\left(-\frac{s^2}{2\sigma^2}\right) \right) ds \right) \\ &= \sqrt{2\pi}\sigma t \operatorname{erf}\left(\frac{t}{\sqrt{2}\sigma}\right) + 2\sigma^2 \left( \exp\left(-\frac{t^2}{2\sigma^2}\right) - \exp\left(-\frac{T^2}{2\sigma^2}\right) \right). \end{aligned}$$

Since  $\exp\left(-\frac{T^2}{2\sigma^2}\right) \rightarrow 0$  as  $T \rightarrow \infty$ , we have:

$$\begin{aligned} \phi_\sigma(t) = (K_\sigma * |\cdot|)(t) &= \lim_{T \rightarrow \infty} C_\sigma(T, t) = \frac{1}{\sqrt{2\pi}\sigma} \sqrt{2\pi}\sigma t \operatorname{erf}\left(\frac{t}{\sqrt{2}\sigma}\right) + \frac{2}{\sqrt{2\pi}\sigma} \sigma^2 \exp\left(-\frac{t^2}{2\sigma^2}\right) \\ &= t \operatorname{erf}\left(\frac{t}{\sqrt{2}\sigma}\right) + \sqrt{\frac{2}{\pi}} \sigma \exp\left(-\frac{t^2}{2\sigma^2}\right). \end{aligned}$$

This proves (2.4). To derive (2.5), we use

$$\frac{d}{dt} \operatorname{erf} \left( \frac{t}{\sqrt{2}\sigma} \right) = \frac{2}{\sqrt{\pi}} \frac{d}{dt} \left[ \int_0^{\left(\frac{t}{\sqrt{2}\sigma}\right)} \exp(-u^2) du \right] = \frac{\sqrt{2}}{\sigma\sqrt{\pi}} \exp \left( -\frac{t^2}{2\sigma^2} \right), \quad (2.6)$$

Plugging in, we get:

$$\begin{aligned} \frac{d}{dt} \phi_\sigma(t) &= \frac{d}{dt} \left( t \operatorname{erf} \left( \frac{t}{\sqrt{2}\sigma} \right) + \sqrt{\frac{2}{\pi}} \sigma \exp \left( -\frac{t^2}{2\sigma^2} \right) \right) \\ &= \operatorname{erf} \left( \frac{t}{\sqrt{2}\sigma} \right) + t \frac{\sqrt{2}}{\sigma\sqrt{\pi}} \exp \left( -\frac{t^2}{2\sigma^2} \right) - \sqrt{\frac{2}{\pi}} \sigma \frac{2t}{2\sigma^2} \exp \left( -\frac{t^2}{2\sigma^2} \right) \\ &= \operatorname{erf} \left( \frac{t}{\sqrt{2}\sigma} \right). \end{aligned}$$

so that (2.5) holds.  $\square$

Next, we review some basic properties of the error function  $\operatorname{erf}(t) = \frac{2}{\sqrt{\pi}} \int_0^t \exp(-s^2) ds$  and the Gaussian integral [1]. It is well known that the Gaussian integral satisfies:

$$\int_{-\infty}^{\infty} \exp(-s^2) ds = 2 \int_0^{\infty} \exp(-s^2) ds = \sqrt{\pi},$$

and, in particular,  $0 < \operatorname{erf}(t) < 1$  for all  $t > 0$ . Using results from [5] on the Gaussian integral, we also have the following bounds for the error function:

**Lemma 2.3** *The error function  $\operatorname{erf}(t) = \frac{2}{\sqrt{\pi}} \int_0^t \exp(-s^2) ds$  satisfies the bounds:*

$$\left(1 - \exp(-t^2)\right)^{\frac{1}{2}} \leq \operatorname{erf}(t) \leq \left(1 - \exp(-2t^2)\right)^{\frac{1}{2}}, \quad \forall t \geq 0. \quad (2.7)$$

**Proof.** In [5], it is shown that for the function  $v(t) := \frac{1}{\sqrt{2\pi}} \int_0^t \exp\left(-\frac{s^2}{2}\right) ds$ , the following bounds hold:

$$\frac{1}{2} \left(1 - \exp\left(-\frac{t^2}{2}\right)\right)^{\frac{1}{2}} \leq v(t) \leq \frac{1}{2} \left(1 - \exp(-t^2)\right)^{\frac{1}{2}}, \quad \forall t \geq 0. \quad (2.8)$$

Now we relate  $v(x)$  to the error function. Using the substitution  $u = \frac{s}{\sqrt{2}}$ :

$$v(t) = \frac{1}{\sqrt{2\pi}} \int_0^{\frac{t}{\sqrt{2}}} \exp(-u^2) \sqrt{2} du = \frac{1}{2} \operatorname{erf} \left( \frac{t}{\sqrt{2}} \right).$$

From (2.8), it follows that:

$$\left(1 - \exp\left(-\frac{x^2}{2}\right)\right)^{\frac{1}{2}} \leq \operatorname{erf} \left( \frac{t}{\sqrt{2}} \right) \leq \left(1 - \exp(-x^2)\right)^{\frac{1}{2}}.$$

Now with the substitution  $s = \frac{x}{\sqrt{2}}$ , (2.7) follows.  $\square$

Using the above properties of the error function and the Gaussian integral, we can prove our convergence result.

**Proposition 2.4** *Let  $g(t) := |t|$  for all  $t \in \mathbb{R}$ , and let the function  $\phi_\sigma := K_\sigma * g$  be defined as in (2.3), for all  $\sigma > 0$ . Then:*

$$\lim_{\sigma \rightarrow 0} \|\phi_\sigma - g\|_{L^1} = 0.$$

**Proof.** By definition of  $\phi_\sigma$ ,

$$\|\phi_\sigma - g\|_{L^1} = \int_{-\infty}^{\infty} |(K_\sigma * |\cdot|)(t) - |t|| dt = 2 \int_0^{\infty} |(K_\sigma * |\cdot|)(t) - t| dt,$$

where the last equality follows from the fact that  $\phi_\sigma - g$  is an even function since both  $\phi_\sigma$  and  $g$  are even functions. Plugging in (2.2), we have:

$$\begin{aligned} \|\phi_\sigma - g\|_{L^1} &= 2 \int_0^{\infty} \left| t \left( \operatorname{erf} \left( \frac{t}{\sqrt{2}\sigma} \right) - 1 \right) + \sqrt{\frac{2}{\pi}} \sigma \exp \left( -\frac{t^2}{2\sigma^2} \right) \right| dt \\ &\leq 2 \int_0^{\infty} \left| t \left( \operatorname{erf} \left( \frac{t}{\sqrt{2}\sigma} \right) - 1 \right) \right| + \sqrt{\frac{2}{\pi}} \sigma \exp \left( -\frac{t^2}{2\sigma^2} \right) dt \\ &= 2 \int_0^{\infty} t \left( 1 - \operatorname{erf} \left( \frac{t}{\sqrt{2}\sigma} \right) \right) + \sqrt{\frac{2}{\pi}} \sigma \exp \left( -\frac{t^2}{2\sigma^2} \right) dt, \end{aligned}$$

where we have used the inequality  $0 < \operatorname{erf}(t) < 1$  for  $t > 0$ . Next, we analyze both terms of the integral. First, using (2.7), we have:

$$(1 - \exp(-t^2))^{\frac{1}{2}} \leq \operatorname{erf}(t) \implies 1 - \operatorname{erf}(t) \leq 1 - (1 - \exp(-t^2))^{\frac{1}{2}} \leq \exp \left( -\frac{t^2}{2} \right),$$

where the last inequality follows from the fact that  $1 - \sqrt{1 - \alpha} \leq \sqrt{\alpha}$  for  $\alpha \in (0, 1)$ . It follows that:

$$\int_0^{\infty} t \left( 1 - \operatorname{erf} \left( \frac{t}{\sqrt{2}\sigma} \right) \right) dt \leq \int_0^{\infty} t \exp \left( -\frac{t^2}{4\sigma^2} \right) dt = 2\sigma^2 \int_0^{\infty} \exp(-u) du = 2\sigma^2,$$

For the second term,

$$\sqrt{\frac{2}{\pi}} \sigma \int_0^{\infty} \exp \left( -\frac{t^2}{2\sigma^2} \right) dt = \sqrt{\frac{2}{\pi}} \sigma \left( \sqrt{2}\sigma \int_0^{\infty} \exp(-s^2) ds \right) = \frac{2}{\sqrt{\pi}} \sigma^2 \frac{\sqrt{\pi}}{2} = \sigma^2.$$

Thus:

$$\lim_{\sigma \rightarrow 0} \|\phi_\sigma - g\|_{L^1} \leq 2 \lim_{\sigma \rightarrow 0} (2\sigma^2 + \sigma^2) = 0.$$

Hence we have that  $\lim_{\sigma \rightarrow 0} \|\phi_\sigma - g\|_{L^1} = 0$ .  $\square$

Note that in the above proof,  $g = |\cdot| \notin L^1$  (since  $g(t) \rightarrow \infty$  as  $t \rightarrow \infty$ ), but the approximation in the  $L^1$  norm still holds. It is likely the approximation result holds for a variety of non-smooth coercive functions  $g$ . Using (2.2), it follows that for the  $\ell_1$  norm, for example, we can use the approximation:

$$\|x\|_1 = \sum_{k=1}^n |x_k| \approx \sum_{k=1}^n \phi_\sigma(x_k) = \sum_{k=1}^n x_k \operatorname{erf}\left(\frac{x_k}{\sqrt{2}\sigma}\right) + \sqrt{\frac{2}{\pi}}\sigma \exp\left(-\frac{x_k^2}{2\sigma^2}\right). \quad (2.9)$$

This approximation is now differentiable at all values of  $x_k$ .

Note from (2.2) that while the approximation  $K_\sigma * |\cdot|$  is indeed smooth, it is positive on  $\mathbb{R}$  and in particular  $(K_\sigma * |\cdot|)(0) = \sqrt{\frac{2}{\pi}}\sigma > 0$ , although  $(K_\sigma * |\cdot|)(0)$  does go to zero as  $\sigma \rightarrow 0$ . To avoid this, we can use instead the following approximation:

$$|t| \approx \phi_\sigma(t) - \phi_\sigma(0) = t \operatorname{erf}\left(\frac{t}{\sqrt{2}\sigma}\right) + \sqrt{\frac{2}{\pi}}\sigma \exp\left(\frac{-t^2}{2\sigma^2}\right) - \sqrt{\frac{2}{\pi}}\sigma, \quad (2.10)$$

which is zero when  $t = 0$ . However, our convergence result with this approximation will not hold. We illustrate the result of the above computations in Figure 3, where we can clearly see that the convolution smooths out the sharp corner of the absolute value, at the expense of being above zero at  $t = 0$  for positive  $\sigma$ .

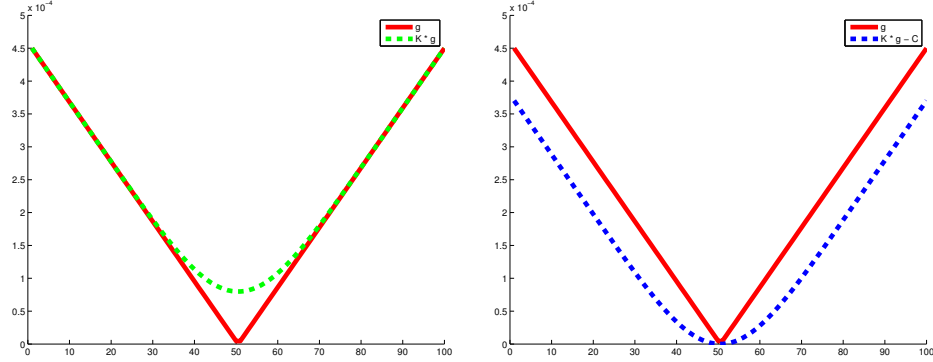


Figure 3: Left: absolute value function  $|t|$  on a fixed interval and the smooth approximation  $|t| \approx \phi_\sigma(t)$  with  $\sigma = 10^{-4}$ . Right: same picture but with the approximation  $\phi_\sigma(t) - \phi_\sigma(0)$  to bring it down to zero at zero.

### 3 Gradient Based Algorithms

In this section, we discuss the use of gradient based optimization algorithms like steepest descent and conjugate gradients in order to approximately minimize the functional (1.1):

$$F_p(x) = \|Ax - b\|_2^2 + 2\tau \left( \sum_{k=1}^n |x_k|^p \right)^{1/p},$$



where we make use of the approximation (2.2) for the non-smooth  $|x_k|$ . Let us first consider the important case of  $p = 1$  leading to the convex  $\ell_1$  norm minimization. In this case, we approximate the non-smooth functional

$$F_1(x) = \|Ax - b\|_2^2 + 2\tau\|x\|_1$$

by the smooth functional:

$$\begin{aligned} H_{1,\sigma}(x) &= \|Ax - b\|_2^2 + 2\tau \sum_{k=1}^n \phi_\sigma(x_k) \\ &= \|Ax - b\|_2^2 + 2\tau \sum_{k=1}^n \left( x_k \operatorname{erf} \left( \frac{x_k}{\sqrt{2}\sigma} \right) + \sqrt{\frac{2}{\pi}} \sigma \exp \left( -\frac{x_k^2}{2\sigma^2} \right) \right). \end{aligned} \quad (3.1)$$

The advantage of working with  $H_{1,\sigma}(x)$  instead of  $F_1(x)$  is that we can easily compute its explicit gradient  $\nabla H_{1,\sigma}(x)$  and even the Hessian  $\nabla^2 H_{1,\sigma}(x)$ :

**Lemma 3.1** *Let  $H_{1,\sigma}(x)$  be as defined in (3.1) where  $A \in \mathbb{R}^{m \times n}$ ,  $b \in \mathbb{R}^m$ ,  $\tau, \sigma > 0$  are constants. Then the gradient is given by:*

$$\nabla H_{1,\sigma}(x) = 2A^T(Ax - b) + 2\tau \begin{bmatrix} \operatorname{erf} \left( \frac{x_1}{\sqrt{2}\sigma} \right) \\ \operatorname{erf} \left( \frac{x_2}{\sqrt{2}\sigma} \right) \\ \vdots \\ \operatorname{erf} \left( \frac{x_n}{\sqrt{2}\sigma} \right) \end{bmatrix}, \quad (3.2)$$

and the Hessian by:

$$\nabla^2 H_{1,\sigma}(x) = 2A^T A + \frac{2\sqrt{2}\tau}{\sigma\sqrt{\pi}} \operatorname{Diag} \left( \exp \left( -\frac{x_1^2}{2\sigma^2} \right), \exp \left( -\frac{x_2^2}{2\sigma^2} \right), \dots, \exp \left( -\frac{x_n^2}{2\sigma^2} \right) \right). \quad (3.3)$$

where  $\operatorname{Diag} : \mathbb{R}^n \rightarrow \mathbb{R}^{n \times n}$  is a diagonal matrix with the input vector elements on the diagonal.

**Proof.** The gradient of  $H_{1,\sigma}(x)$  is given by:

$$\begin{aligned} \nabla H_{1,\sigma}(x) &= 2A^T(Ax - b) \\ &\quad + 2\tau \left\{ \frac{d}{dx_k} \left( x_k \operatorname{erf} \left( \frac{x_k}{\sqrt{2}\sigma} \right) + \sqrt{\frac{2}{\pi}} \sigma \exp \left( -\frac{x_k^2}{2\sigma^2} \right) \right) \right\}_{k=1}^n, \end{aligned}$$

Using (2.5), we have that:

$$\begin{aligned} \frac{d}{dt} \operatorname{erf} \left( \frac{t}{\sqrt{2}\sigma} \right) &= \frac{\sqrt{2}}{\sigma\sqrt{\pi}} \exp \left( -\frac{t^2}{2\sigma^2} \right) \implies \frac{d}{dx_k} \left( x_k \operatorname{erf} \left( \frac{x_k}{\sqrt{2}\sigma} \right) + \sqrt{\frac{2}{\pi}} \sigma \exp \left( -\frac{x_k^2}{2\sigma^2} \right) \right) \\ &= \operatorname{erf} \left( \frac{x_k}{\sqrt{2}\sigma} \right) + x_k \frac{\sqrt{2}}{\sigma\sqrt{\pi}} \exp \left( -\frac{x_k^2}{2\sigma^2} \right) - \sqrt{\frac{2}{\pi}} \sigma \frac{2x_k}{2\sigma^2} \exp \left( -\frac{x_k^2}{2\sigma^2} \right) = \operatorname{erf} \left( \frac{x_k}{\sqrt{2}\sigma} \right) \end{aligned}$$

so (3.2) holds. For the Hessian matrix, we have:

$$\nabla^2 H_{1,\sigma}(x) = 2A^T A + 2\tau \text{Diag} \left( \frac{d}{dx_1} \text{erf} \left( \frac{x_1}{\sqrt{2}\sigma} \right), \frac{d}{dx_2} \text{erf} \left( \frac{x_2}{\sqrt{2}\sigma} \right), \dots, \frac{d}{dx_n} \text{erf} \left( \frac{x_n}{\sqrt{2}\sigma} \right) \right),$$

and using (2.6), we obtain (3.3).  $\square$

Next, we discuss the smooth approximation to the general functional (1.1). In particular, we are interested in the case  $p < 1$ . In this case, the functional is not convex, but may still be useful in compressive sensing applications [4]. The approximating functional using  $\phi_\sigma$  from (2.3) becomes:

$$\begin{aligned} H_{p,\sigma}(x) &:= \|Ax - b\|_2^2 + 2\tau \left( \sum_{k=1}^n \phi_\sigma(x_k)^p \right)^{1/p} \\ &= \|Ax - b\|_2^2 + 2\tau \left( \sum_{k=1}^n \left( x_k \text{erf} \left( \frac{x_k}{\sqrt{2}\sigma} \right) + \sqrt{\frac{2}{\pi}} \sigma \exp \left( \frac{-x_k^2}{2\sigma^2} \right) \right)^p \right)^{1/p}. \end{aligned} \quad (3.4)$$

**Lemma 3.2** *Let  $H_{p,\sigma}(x)$  be as defined in (3.4) where  $p > 0$  and  $\sigma > 0$ . Then the gradient is given by:*

$$\nabla H_{p,\sigma}(x) = 2A^T(Ax - b) + 2\tau p \left( \sum_{k=1}^n \phi_\sigma(x_k)^p \right)^{(1-p)/p} \left\{ \phi_\sigma(x_j)^{p-1} \text{erf} \left( \frac{x_j}{\sqrt{2}\sigma} \right) \right\}_{j=1}^n, \quad (3.5)$$

and the Hessian is given by:

$$\nabla^2 H_{p,\sigma}(x) = 2A^T A + 2\tau \left( v(x)v(x)^T + \text{Diag}(w(x)) \right), \quad (3.6)$$

where the functions  $v, w : \mathbb{R}^n \rightarrow \mathbb{R}^n$  are defined for all  $x \in \mathbb{R}^n$ :

$$\begin{aligned} v(x) &:= \left\{ \sqrt{1-p} \phi_\sigma(x_j)^{p-1} \text{erf} \left( \frac{x_j}{\sqrt{2}\sigma} \right) \left( \sum_{k=1}^n \phi_\sigma(x_k)^p \right)^{(1-2p)/(2p)} \right\}_{j=1}^n, \\ w(x) &:= \left( \sum_{k=1}^n \phi_\sigma(x_k)^p \right)^{(1-p)/p} \left\{ (p-1) \phi_\sigma(x_j)^{p-2} \left( \text{erf} \left( \frac{x_j}{\sqrt{2}\sigma} \right) \right)^2 + \frac{\sqrt{2}}{\sigma\sqrt{\pi}} \phi_\sigma(x_j)^{p-1} \exp \left( -\frac{x_j^2}{2\sigma^2} \right) \right\}_{j=1}^n. \end{aligned}$$

**Proof.** Define  $G_{p,\sigma} : \mathbb{R}^n \rightarrow \mathbb{R}$  by

$$G_{p,\sigma}(x) := \left( \sum_{k=1}^n \phi_\sigma(x_k)^p \right)^{1/p}. \quad (3.7)$$

Then  $H_{p,\sigma}(x) = \|Ax - b\|^2 + 2\sigma G_{p,\sigma}(x)$  for all  $x$ , and for each  $j = 1, \dots, n$ ,

$$\frac{\partial}{\partial x_j} G_{p,\sigma}(x) = \frac{1}{p} \left( \sum_{k=1}^n \phi_\sigma(x_k)^p \right)^{(1-p)/p} \left( p \phi_\sigma(x_j)^{p-1} \phi'_\sigma(x_j) \right) = G_{p,\sigma}(x)^{1-p} \phi_\sigma(x_j)^{p-1} \text{erf} \left( \frac{x_j}{\sqrt{2}\sigma} \right) \quad (3.8)$$

where we have used (2.5). Hence, (3.5) follows. Next, we compute the Hessian of  $G_{p,\sigma}$ . For each  $i \neq j$ ,

$$\begin{aligned}
\frac{\partial^2}{\partial x_i \partial x_j} G_{p,\sigma}(x) &= \frac{\partial}{\partial x_i} \left[ G_{p,\sigma}(x)^{1-p} \phi_\sigma(x_j)^{p-1} \operatorname{erf} \left( \frac{x_j}{\sqrt{2}\sigma} \right) \right] \\
&= (1-p) \phi_\sigma(x_j)^{p-1} \operatorname{erf} \left( \frac{x_j}{\sqrt{2}\sigma} \right) G_{p,\sigma}(x)^{-p} \frac{\partial}{\partial x_i} G_{p,\sigma}(x) \\
&= (1-p) \phi_\sigma(x_i)^{p-1} \phi_\sigma(x_j)^{p-1} \operatorname{erf} \left( \frac{x_i}{\sqrt{2}\sigma} \right) \operatorname{erf} \left( \frac{x_j}{\sqrt{2}\sigma} \right) G_{p,\sigma}(x)^{1-2p} \\
&= v(x)_i v(x)_j = (v(x) v(x)^T)_{ij},
\end{aligned}$$

and when  $i = j$ , for each  $j = 1, \dots, n$ ,

$$\begin{aligned}
\frac{\partial^2}{\partial^2 x_j} G_{p,\sigma}(x) &= \frac{\partial}{\partial x_j} \left[ G_{p,\sigma}(x)^{1-p} \phi_\sigma(x_j)^{p-1} \operatorname{erf} \left( \frac{x_j}{\sqrt{2}\sigma} \right) \right] \\
&= (1-p) \phi_\sigma(x_j)^{2(p-1)} \left( \operatorname{erf} \left( \frac{x_j}{\sqrt{2}\sigma} \right) \right)^2 G_{p,\sigma}(x)^{1-2p} \\
&\quad + G_{p,\sigma}(x)^{1-p} \left( (p-1) \phi_\sigma(x_j)^{p-2} \left( \operatorname{erf} \left( \frac{x_j}{\sqrt{2}\sigma} \right) \right)^2 + \frac{\sqrt{2}}{\sigma\sqrt{\pi}} \phi_\sigma(x_j)^{p-1} \exp \left( -\frac{x_j^2}{2\sigma^2} \right) \right) \\
&= v(x)_j^2 + w(x)_j = (v(x) v(x)^T + \operatorname{Diag}(w(x)))_{jj}.
\end{aligned}$$

Hence, (3.6) holds.  $\square$

Given  $H_{p,\sigma}(x) \approx F_p(x)$  and  $\nabla H_{p,\sigma}(x)$ , we can apply a number of gradient based methods for the minimization of  $H_{p,\sigma}(x)$  (and hence for the approximate minimization of  $F_p(x)$ ), which take the following general form:

---

**Algorithm 1:** Generic Gradient Method for finding  $\arg \min H_{p,\sigma}(x)$ .

---

```

Pick an initial point  $x^0$ ;
for  $k = 0, 1, \dots$ , maxiter do
    Compute search direction  $s^k$  based on gradient  $\nabla H_{p,\sigma}(x^k)$ . ;
    Compute step size parameter  $\mu$  via line search. ;
    Update the iterate:  $x^{k+1} = x^k + \mu s^k$ . ;
    Check if the termination conditions are met. ;
end
Record final solution:  $\bar{x} = x^{k+1}$ . ;

```

---

Note that in the case of  $p < 1$ , the functional  $F_p(x)$  is not convex, so such an algorithm may not converge to the global minimum in that case. The generic algorithm above depends on the choice of search direction  $s^k$ , which is based on the gradient, and the line search, which can be performed several different ways.

### 3.1 Line Search Techniques

Gradient based algorithms differ based on the choice of search direction vector  $s^k$  and line search techniques for parameter  $\mu$ . In this section we describe some suitable line search techniques. Given the current iterate  $x^k$  and search direction  $s^k$ , we would like to choose  $\mu$  so that:

$$H_{p,\sigma}(x^{k+1}) = H_{p,\sigma}(x^k + \mu s^k) \leq H_{p,\sigma}(x^k),$$

where  $\mu > 0$  is a scalar which measures how long along the search direction we advance from the previous iterate. Ideally, we would like a strict inequality and the functional value to decrease. Exact line search would solve the single variable minimization problem:

$$\bar{\mu} = \arg \min_{\mu} H_{p,\sigma}(x^k + \mu s^k).$$

The first order necessary optimality condition (i.e.,  $\nabla H_{p,\sigma}(x + \mu s)^T s = 0$ ) can be used to find a candidate value for  $\mu$ , but it is not easy to solve the gradient equation.

An alternative approach is to use a backtracking line search to get a step size  $\mu$  that satisfies one or two of the Wolfe conditions [12]. A typical backtracking line search algorithm proceeds as follows:

---

**Algorithm 2:** Backtracking Line Search

---

**Input** : Evaluators for  $H_{p,\sigma}(x)$  and  $\nabla H_{p,\sigma}(x)$ , current iterate  $x^k$ , search direction  $s^k$ , and constants  $\mu > 0$ ,  $\rho \in (0, 1)$ ,  $c \in (0, 1)$ .

**Output:**  $\mu > 0$  satisfying a sufficient decrease condition.

**while**  $H_{p,\sigma}(x^k + \mu s^k) > H_{p,\sigma}(x^k) + c\mu(\nabla H_{p,\sigma}(x^k))^T s^k$  **do**  
 $\mu = \rho\mu$ ;  
**end**

---

This update scheme can be slow since several evaluations of  $H_{p,\sigma}(x)$  may be necessary, which are relatively expensive when the dimension  $n$  is large. It also depends on the choice of parameters  $\rho$  and  $c$ , to which the generic gradient method may be sensitive.

Another way to perform approximate line search is to utilize a Taylor series approximation for the solution of  $\frac{d}{d\mu} H_{p,\sigma}(x + \mu s) = 0$  [15]. This involves the gradient and Hessian terms which we have previously computed. Using the second order Taylor approximation of  $g(t) := H_{p,\sigma}(x + ts)$  at any given  $x, s \in \mathbb{R}^n$ , we have that

$$g'(t) = g'(0) + tg''(0) + o(t) \approx g'(0) + tg''(0); \quad (3.9)$$

using basic matrix calculus:

$$\begin{aligned} g'(t) &= (\nabla H_{p,\sigma}(x + ts))^T s \implies g'(0) = \nabla H_{p,\sigma}(x)^T s \\ g''(t) &= \left[ (\nabla^2 H_{p,\sigma}(x + ts))^T s \right]^T s = s^T \nabla^2 H_{p,\sigma}(x + ts) s \implies g''(0) = s^T \nabla^2 H_{p,\sigma}(x) s, \end{aligned}$$

we get that  $g'(0) + \mu g''(0) = 0$  if and only if

$$\mu = -\frac{\nabla H_{p,\sigma}(x)^T s}{s^T \nabla^2 H_{p,\sigma}(x) s}, \quad (3.10)$$

which can be used as the step size in Algorithm 1.

For the case  $p = 1$  (approximating the  $\ell_1$  functional), the Hessian is  $A^T A$  plus a diagonal matrix, which is quick to form and the above approximation can be efficiently used for line search. For  $p \neq 1$ , the Hessian is the sum of  $A^T A$  and  $M$ , and  $M$  in turn is the sum of a diagonal matrix and a rank one matrix; the matrix-vector multiplication involving this Hessian is slightly more expensive than in the case  $p = 1$ . In this case, one may approximate the Hessian in (3.10) using finite differences, i.e., when  $\xi > 0$  is sufficiently small,

$$g''(t) \approx \frac{g'(t + \xi) - g'(t - \xi)}{2\xi}. \implies g''(0) \approx \frac{g'(\xi) - g'(-\xi)}{2\xi} \quad (3.11)$$

Approximating  $g''(0)$  in (3.9) by  $\frac{g'(\xi) - g'(-\xi)}{2\xi}$ , we get

$$\frac{d}{d\mu} H_{p,\sigma}(x + \mu s) \approx \nabla H_{p,\sigma}(x)^T s + \mu \frac{(\nabla H_{p,\sigma}(x + \xi s) - \nabla H_{p,\sigma}(x - \xi s))^T s}{2\xi}. \quad (3.12)$$

Setting the right hand side of (3.12) to zero, and solving for  $\mu$ , we get

$$\mu = \frac{-2\xi \nabla H_{p,\sigma}(x)^T s}{(\nabla H_{p,\sigma}(x + \xi s) - \nabla H_{p,\sigma}(x - \xi s))^T s}. \quad (3.13)$$

In practice, we find that for  $p = 1$ , the Hessian based line search (3.10) works well; for  $p \neq 1$ , one can also use the finite difference scheme (3.13) if one wants to avoid evaluating the Hessian. In the finite difference scheme, the parameter  $\xi$  should be taken to be of the same order as the components of the current iterate  $x^k$ .

### 3.2 Steepest Descent and Conjugate Gradient Algorithms

We now present steepest descent and conjugate gradient schemes, in Algorithms 3 and 4 respectively, which can be used for sparsity constrained regularization. We remark again that the choice of sparsity constrained regularization is just one possible application of the smoothing technique we have presented. Steepest descent and conjugate gradient methods differ in the choice of the search direction. In steepest descent methods, we simply take the negative of the gradient as the search direction. For nonlinear conjugate gradient methods, which one expects to perform better than steepest descent, several different search direction updates are possible. We find that the Polak-Ribière scheme often offers good performance [13, 14, 15]. In this scheme, we set the initial search direction  $s^0$  to the negative gradient, as in steepest descent, but then do a more complicated update involving the gradient

at the current and previous steps:

$$\begin{aligned}\beta^{k+1} &= \max \left\{ \frac{\nabla H_{p,\sigma_k}(x^{k+1})^T (\nabla H_{p,\sigma_k}(x^{k+1}) - \nabla H_{p,\sigma_k}(x^k))}{\nabla H_{p,\sigma_k}(x^k)^T \nabla H_{p,\sigma_k}(x^k)}, 0 \right\}, \\ s^{k+1} &= -\nabla H_{p,\sigma_k}(x^{k+1}) + \beta^{k+1} s^k.\end{aligned}$$

One extra step we introduce in Algorithms 3 and 4 below is a thresholding which sets small components to zero. That is, at the end of each iteration, we retain only a portion of the largest coefficients. This is necessary, as otherwise the solution we recover will contain many small noisy components and will not be sparse. In our numerical experiments, we found that soft thresholding works well when  $p = 1$  and that hard thresholding works well when  $p < 1$ . The componentwise soft and hard thresholding functions with parameter  $\tau > 0$  are given by:

$$(S_\tau(x))_k = \begin{cases} x_k - \tau, & x_k \geq \tau \\ 0, & -\tau \leq x_k \leq \tau \\ x_k + \tau, & x_k \leq -\tau \end{cases}; \quad (H_\tau(x))_k = \begin{cases} x_k, & |x_k| > \tau \\ 0, & -\tau \leq x_k \leq \tau \end{cases}, \quad \forall x \in \mathbb{R}^n. \quad (3.14)$$

Note that we also choose to vary the parameter  $\sigma$  in the approximating function  $\phi_\sigma$  (defined in (2.4)), starting relatively far from zero and decreasing at each iteration. The decrease can be controlled by a parameter  $\alpha \in (0, 1)$  so that  $\sigma_{k+1} = \alpha \sigma_k$ . The choice  $\alpha = 0.5$  works well in our application. We could also tie  $\sigma^n$  to the progress of the iteration, such as the quantity  $\|x^{k+1} - x^k\|_2$ . One should experiment to find what works best with a given application. We choose to decrease  $\sigma$  in a fixed fraction so that we progress from a numerically smooth to a numerically sharper corner gradually for the approximation to the absolute value function as  $\sigma \rightarrow 0$ .

Finally, we comment on the computational cost of Algorithms 3 and 4, relative to standard iterative thresholding methods, notably the FISTA method. The FISTA iteration for  $F_1(x)$ , for example, would be implemented as:

$$y^0 = x^0, \quad x^{k+1} = S_\tau(y^k + A^T b - A^T A y^k), \quad y^{k+1} = x^{k+1} + \frac{t_k - 1}{t_{k+1}} (x^{k+1} - x^k), \quad (3.15)$$

where  $\{t_k\}_k$  is a special sequence of constants [2]. For large linear systems, the main cost is in the evaluation of  $A^T A y^n$ . The same is true for the gradient based schemes we present below. The product of  $A^T A$  and the vector iterate goes into the gradient computation and the line search method (note that it just needs to be computed once per iteration). Notice also that the gradient and line search computations involve the evaluation of the error function  $\text{erf}(t) = \frac{2}{\sqrt{\pi}} \int_0^t e^{-u^2} du$ , and there is no closed form solution for this integral. However, various ways of efficiently approximating the integral value exist: apart from standard quadrature methods, several approximations involving the exponential function are described in [1]. The gradient methods below do have extra overhead compared to the thresholding schemes and may not be ideal for runs with large numbers of iterations. However, for large matrices, the runtimes are competitive, since the most time consuming step (multiplication with  $A^T A$ ) is common to both.

Algorithm 3, below, presents a simple steepest descent scheme to approximately minimize  $F_p$  defined in (1.1). The function **Threshold** $(\cdot, \tau)$  in the algorithm refers to either one of the two thresholding functions defined in (3.14).

---

**Algorithm 3:** Steepest Descent Scheme

---

**Input** : An  $m \times n$  matrix  $A$ , an initial guess  $n \times 1$  vector  $x^0$ , a parameter  $\tau < \|A^T b\|_\infty$ , a parameter  $p \in (0, 1]$ , a parameter  $\sigma_0 > 0$ , a parameter  $0 < \alpha < 1$ , the maximum number of iterations  $M$ , and a routine to evaluate the gradient  $\nabla H_{p,\sigma}(x)$  (and possibly the Hessian  $\nabla^2 H_{p,\sigma}(x)$  depending on choice of line search method).

**Output:** A vector  $\bar{x}$ , close to either the global or local minimum of  $F_p(x)$ , depending on choice of  $p$ .

```
for  $k = 0, 1, \dots, M$  do
   $s^k = -\nabla H_{p,\sigma_k}(x^k)$  ;
  use line search to find  $\mu > 0$ ;
   $x^{k+1} = \text{Threshold}(x^k + \mu s^k, \tau)$  ;
   $\sigma_{k+1} = \alpha \sigma_k$  ;
end
 $\bar{x} = x^{k+1}$ ;
```

---

Next, we present a nonlinear Polak-Ribière conjugate gradient scheme to approximately minimize  $F_p$  [13, 14, 15], in Algorithm 4 below. In practice, this slightly more complicated algorithm is expected to perform better than the simple steepest descent method.

---

**Algorithm 4:** Nonlinear Conjugate Gradient Scheme

---

**Input** : An  $m \times n$  matrix  $A$ , an initial guess  $n \times 1$  vector  $x^0$ , a parameter  $\tau < \|A^T b\|_\infty$ , a parameter  $p \in (0, 1]$ , a parameter  $\sigma_0 > 0$ , a parameter  $0 < \alpha < 1$ , the maximum number of iterations  $M$ , and a routine to evaluate the gradient  $\nabla H_{p,\sigma}(x)$  (and possibly the Hessian  $\nabla^2 H_{p,\sigma}(x)$  depending on choice of line search method)..

**Output:** A vector  $\bar{x}$ , close to either the global or local minimum of  $F_p(x)$ , depending on choice of  $p$ .

```
 $s^0 = -\nabla H_{p,\sigma_0}(x^0)$  ;
for  $k = 0, 1, \dots, M$  do
  use line search to find  $\mu > 0$ ;
   $x^{k+1} = \text{Threshold}(x^k + \mu s^k, \tau)$  ;
   $\beta^{k+1} = \max \left\{ \frac{\nabla H_{p,\sigma_k}(x^{k+1})^T (\nabla H_{p,\sigma_k}(x^{k+1}) - \nabla H_{p,\sigma_k}(x^k))}{\nabla H_{p,\sigma_k}(x^k)^T \nabla H_{p,\sigma_k}(x^k)}, 0 \right\}$  ;
   $s^{k+1} = -\nabla H_{p,\sigma_k}(x^{k+1}) + \beta^{k+1} s^k$  ;
   $\sigma_{k+1} = \alpha \sigma_k$  ;
end
 $\bar{x} = x^{k+1}$ ;
```

---

## 4 Numerical Experiments

We now show some numerical experiments, comparing Algorithm 4 with FISTA, a state of the art sparse regularization algorithm [2] outlined in (3.15). We use our CG scheme with  $p = 1$  in most experiments for direct comparison with FISTA results, but also include an example with  $p < 1$ . We present plots of averaged quantities over many trials, wherever possible. We observe that for these experiments, the CG scheme gives good results in few iterations, although each iteration of CG is more expensive than a single iteration of an iterative thresholding algorithm like FISTA.

In Figure 4 on Page 18, we present plots for the case of a mildly ill-conditioned matrix comparing the performance of FISTA and CG for a fixed  $\tau$ . We run 20 trials of 30 iterations each for a  $1000 \times 1000$  ill-conditioned matrix formed using a randomized reverse SVD procedure. We generate a sparse signal  $x$  with 1% nonzeros, then form  $b = Ax + e$  ( $e$  being the noise vector) with 10% noise level in relation to the norm of  $Ax$ . For the algorithms, we set  $\tau$  (used in either one of the thresholding functions defined in (3.14)) to be a fixed fraction  $\frac{1}{500}$  of  $\|A^T b\|_\infty$ , i.e.,  $\tau = \frac{\|A^T b\|_\infty}{500}$  (only one  $\tau$  value is used in this test), starting from a zero initial guess and iteratively minimize the  $\ell_1$  functional  $F_1(x) = \|Ax - b\|_2^2 + 2\tau\|x\|_1$  using FISTA and our CG scheme. We observe from Figure 4 that our CG scheme decreases the functional faster and gets to a lower percent error faster producing a suitable reconstruction in few iterations. In this figure, the functional values and percent error curves we present are averaged over 20 trials with a randomly constructed matrix of given conditioning. In general, we observe that CG tends to produce good results in few iterations, especially when the noise level in  $b$  is relatively high. FISTA takes more iterations to reach a better solution in such circumstances.

In practice, when performing a sparse reconstruction, we typically vary the value of the regularization parameter  $\tau$  and move along a regularization parameter curve while doing warm starts, starting from a relatively high value of  $\tau$  close to  $\|A^T b\|_\infty$  with a zero initial guess (since for  $\tau > \|A^T b\|_\infty$ , the  $\ell_1$  minimizer is zero) and moving to a lower value, while reusing the solution at the previous  $\tau$  as the initial guess at the next, lower  $\tau$  [10, 17]. If the  $\tau$ 's follow a logarithmic decrease, the corresponding curves we observe are like those plotted in Figure 5. At some  $\tau$ , the reconstruction  $x_\tau$  will be optimal along the curve and the percent error between solution  $x_\tau$  and solution  $x$  will be lowest. However, since we do not know the true solution  $x$  we have to use other criteria to pick the  $\tau$  at which we want to record the solution. One way is by using the norm of the noise vector in the right hand side  $\|e\|_2$ . If an accurate estimate of this is known, we can use the solution at the  $\tau$  for which the residual norm  $\|Ax_\tau - b\|_2 \approx \|e\|_2$ . In Figure 5 we plot the residuals vs  $\tau$  for the two algorithms along with the noise norm line; the intersection occurs roughly at the same point for both algorithms. We also plot curves for the percent errors  $100 \frac{\|x_\tau - x\|_2}{\|x\|_2}$  and the functional values  $F_1(x_\tau)$  vs  $\tau$  (note that CG is in fact minimizing an approximation to the non-smooth  $F_1(x)$ , yet the value of  $F_1(x)$  for the algorithm is still competitive with FISTA). For this choice of parameters (10 percent nonzeros in  $x$  and 10 percent noise level in  $b$ ) we see that the absolute minimum values of the curves are lower for CG, although at the noise curve intersecting  $\tau$  the quantities for the two algorithms are similar. The curves shown are averages over 20 runs for matrices with the same conditioning as in Figure 4.

We present more general contour plots in Figure 6 which compare the performance of the two algorithms at different combinations of number of nonzeros and noise levels. We show contour plots for two types of errors: absolute minimum errors over the regularization curve at each combination



and errors recorded at the  $\tau$  for which  $\|Ax_\tau - b\|_2$  is closest to  $\|e\|_2$ . The data at each point of the contour plots is obtained by running FISTA and CG for same number of iterations (30) at each  $\tau$  starting from  $\tau = \frac{\|A^T b\|_\infty}{10}$  going down to  $\tau = \frac{\|A^T b\|_\infty}{50000}$  and reusing the previous solution as the initial guess at the next  $\tau$ . We then record the minimum percent error (best  $x_\tau$  amongst all  $\tau$  sampled) and the percent error for the  $\tau$  closest to the noise intersection curve point. We do this for 20 trials and record the averaged values. From Figure 6 we observe that as the noise level in  $b$  becomes higher, CG does better in the same number of iterations if the number of nonzeros remains low, as the noise level in  $b$  increases. However as the number of nonzeros increases, the performance is similar to FISTA.

Finally, we do a compressive sensing image recovery test by trying to recover the original image from its samples. A sparse image  $x$  was used to construct the right hand side with a sensing matrix  $A$  via  $b = Ax + e$  with  $e$  being the noise vector with 10 percent noise level relative to the norm of  $b$ . The matrices  $A$  were random from the normal distribution with different numbers of rows (1400, 2100, 2800, and 3500). The number of columns and image pixels was 5025. We try to recovery  $x$  given the sensing matrix  $A$  and the noisy measurements  $b$ . In each trial, we solved approximately

$$\bar{x} = \arg \min_x \left\{ \|Ax - b\|_2^2 + 2\tau \left( \sum_{k=1}^n |x_k|^p \right)^{\frac{1}{p}} \right\}$$
 at a fixed  $\tau$  for each algorithm with  $p = 1$  for FISTA and CG and then with  $p = 0.92$  with CG. The results are shown in Figure 7 on Page 20.

In the experiments, we implemented CG as in Algorithm 4, with the Hessian based line search approximation (3.10) and soft thresholding (3.14) for  $p = 1$  and with the finite difference line search approximation (3.13) and hard thresholding (3.14) for  $p < 1$ .

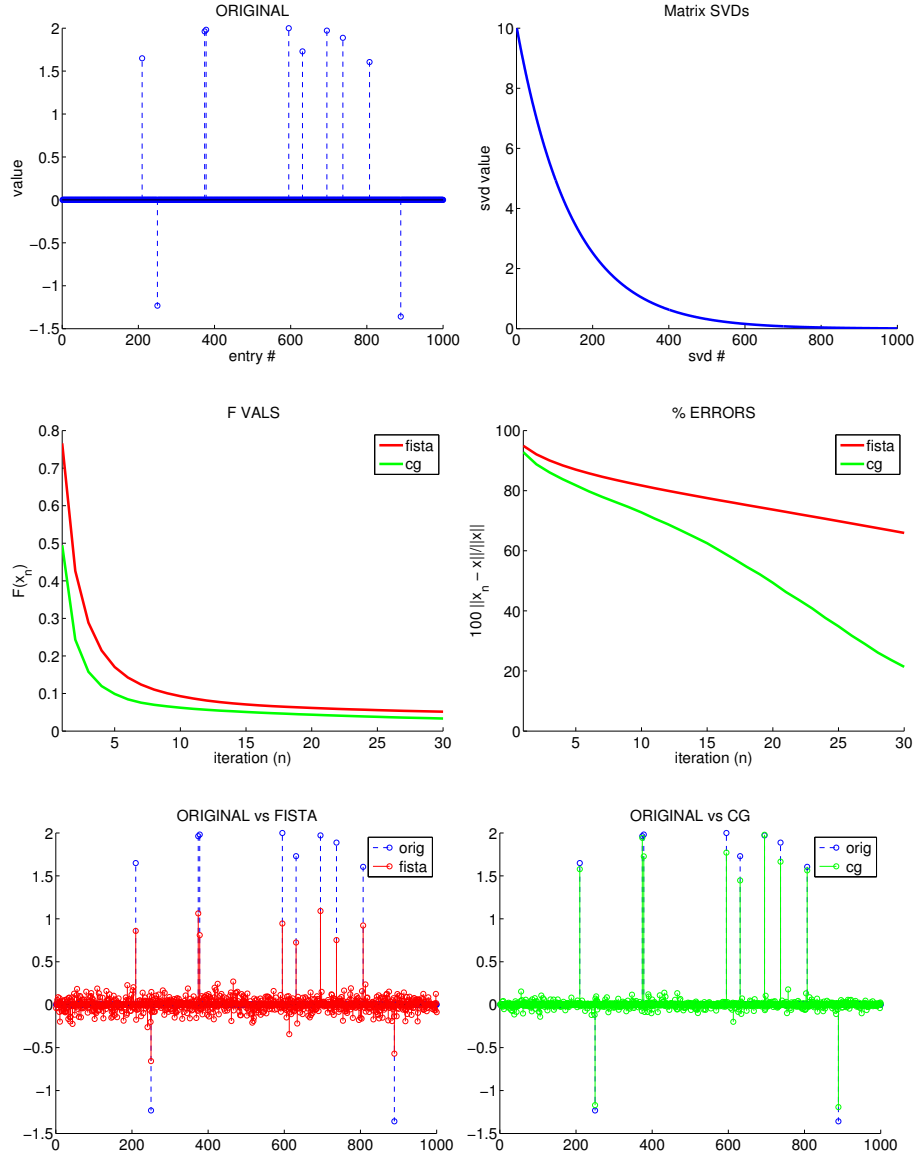


Figure 4: Results for a single fixed  $\tau$  with zero initial guess. Row 1: original signal and singular values profile of the matrix (from one trial). Row 2: values of  $F_1(x^n)$  vs iteration and percent errors  $100 \frac{\|x^n - x\|_2}{\|x\|_2}$  vs iteration (averaged values over several trials). Row 3: reconstructed solutions with FISTA and CG after 30 iterations (from one trial).

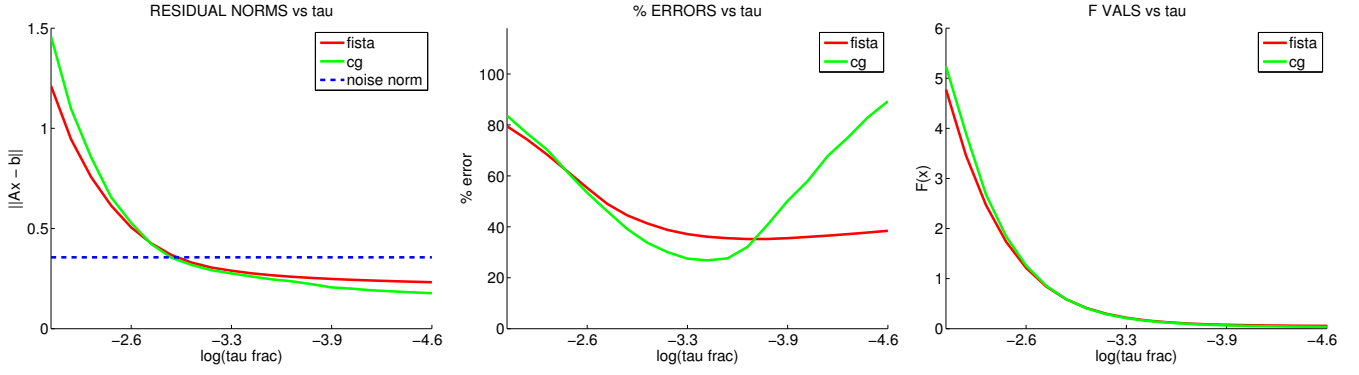


Figure 5: Averaged quantities along the regularization curve. Residual norms  $\|Ax_\tau - b\|_2$ , percent errors  $100 \frac{\|x_\tau - x\|_2}{\|x\|_2}$ , and  $\ell_1$  functional values  $F_1(x_\tau)$  versus decreasing  $\tau$  (fraction of  $\|A^T b\|_\infty$ ) for FISTA and CG.

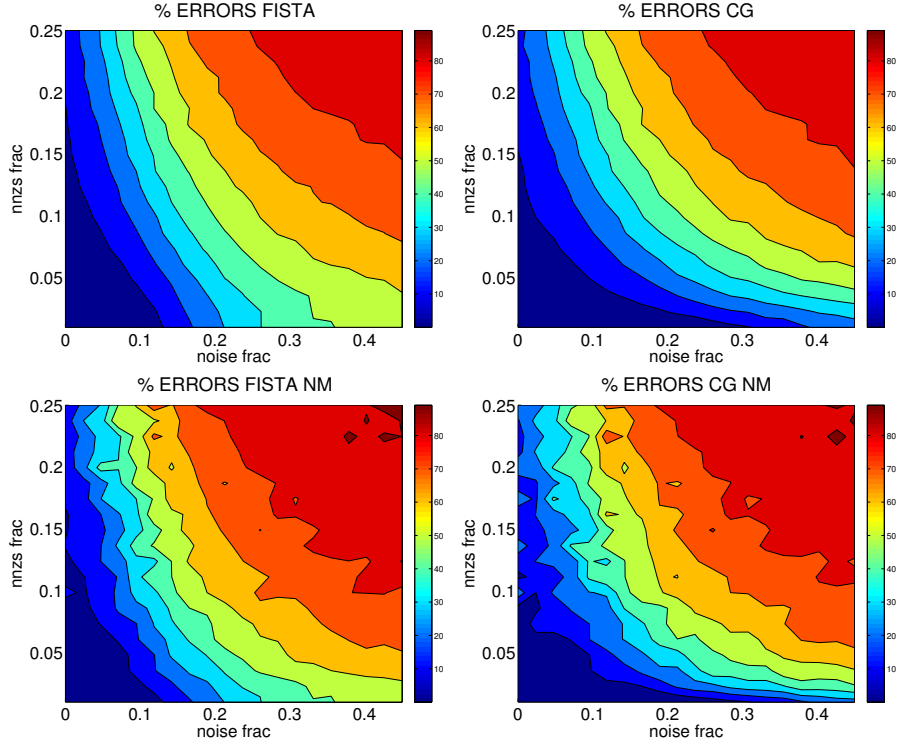


Figure 6: Contour plots for different combinations of nonzeros and noise fractions. First row plots show minimum percent errors over all  $\tau$ s along the regularization curve and second row plots show percent errors at the value of  $\tau$  along the curve for which  $\|Ax_\tau - b\|_2$  is closest to  $\|e\|_2$  (noise match).

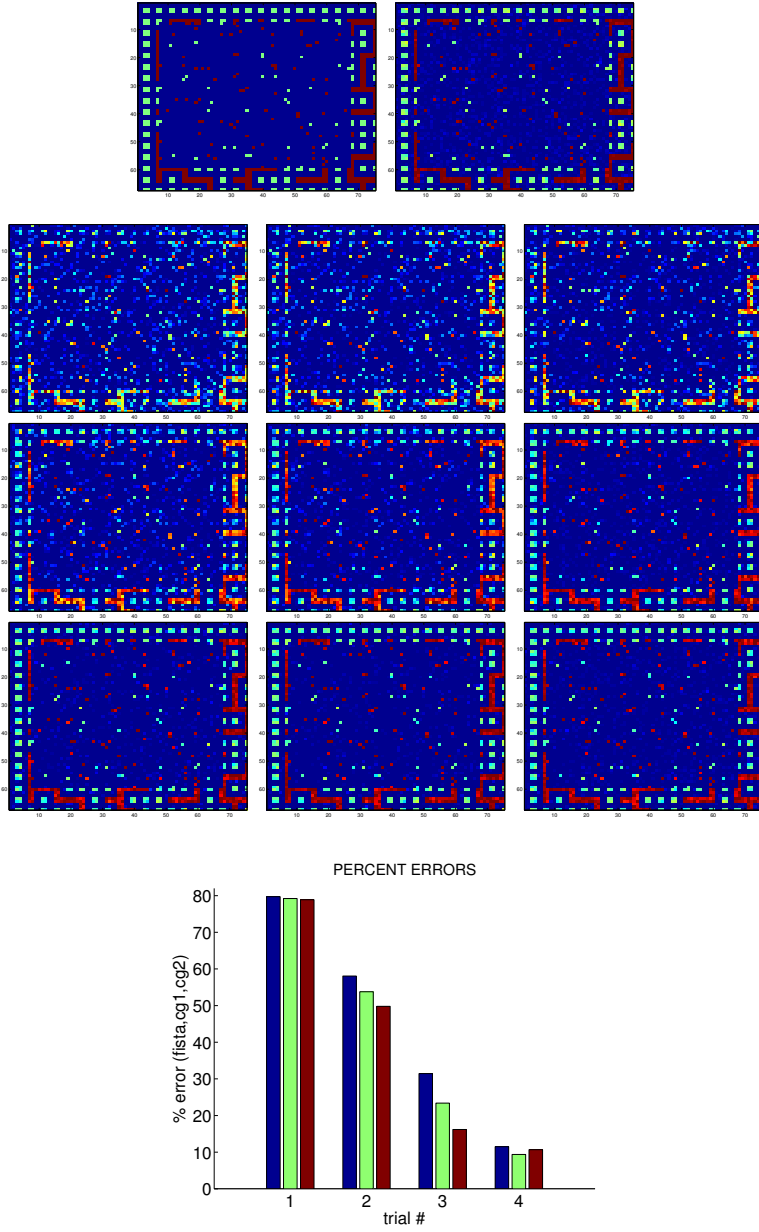


Figure 7: Image reconstruction sampled via random sensing matrices with different numbers of rows. Row 1: original and noisy image. Rows 2,3,4: recovered images using FISTA, CG (with  $p = 1$ ), and CG (with  $p = 0.92$ ) run for 30 iterations with 1400, 2100, 2800, and 3500 samples (sensing matrix rows). Row 5: bar plot of percent errors for the three methods for each number of samples.

## 5 Conclusions

In this article, we discuss a smoothing approach useful for non-smooth regularization, such as sparse regularization, in which a non-differentiable term appears. In the case of sparse regularization, this is the absolute value function  $g(t) = |t|$ . For smoothing, we use a convolution with an approximate mollifier. We construct a smooth approximation to  $g(t)$  and establish convergence results for our approximation in the  $L^1$  norm. This allows us to construct a smooth approximation to the original non-smooth functional  $F_p(x)$  (of which the popular  $\ell_1$  functional is a special case for  $p = 1$ ) and to compute the gradient of this approximating functional to use gradient based methods like steepest descent and conjugate gradients.

Many existing algorithms for sparse regularization rely on iterative thresholding algorithms. Many of these schemes involve some modification of the Landweber iteration scheme, paired with thresholding. Landweber iteration is a classical but slowly converging algorithm and we find that more advanced full gradient based methods, though operating on the approximate functional/gradient pair  $H_{p,\sigma}(x)$ ,  $\nabla H_{p,\sigma}(x)$ , instead of the original non-smooth functional  $F_p(x)$ , tend to be competitive relative to the iterative thresholding schemes.

We observe from the numerics in Section 4 that in many cases, in a small number of iterations, we are able to obtain better results than FISTA can for the  $\ell_1$  case (for example, in the presence of high noise). We also observe that when  $p < 1$  but not too far away from one (say  $p \approx 0.9$ ) we can sometimes obtain even better reconstructions in compressed sensing experiments.

The simple algorithms we show maybe useful for larger problems, where iteration count is important, or where one wants to obtain a rough solution (for example, to warm start a thresholding based method) in few iterations. Moreover the ideas presented here can be extended to design more complex algorithms, possibly with better performance for ill-conditioned problems, by exploiting the wealth of available literature on conjugate gradient and other gradient based methods. Finally, the convolution smoothing technique which we use is more flexible than the traditional mollifier approach and maybe useful in a variety of applications where the minimization of non-smooth functions is necessary.

## References

- [1] Milton Abramowitz and Irene A. Stegun, editors. *Handbook of mathematical functions with formulas, graphs, and mathematical tables*. A Wiley-Interscience Publication. John Wiley & Sons, Inc., New York; National Bureau of Standards, Washington, DC, 1984.
- [2] Amir Beck and Marc Teboulle. A fast iterative shrinkage-thresholding algorithm for linear inverse problems. *SIAM J. Imaging Sci.*, 2(1):183–202, 2009.
- [3] Rick Chartrand. Fast algorithms for nonconvex compressive sensing: Mri reconstruction from very few data. In *Int. Symp. Biomedical Imaging*, 2009.
- [4] Rick Chartrand and Valentina Staneva. Restricted isometry properties and nonconvex compressive sensing. *Inverse Problems*, 24(3):035020, 14, 2008.
- [5] John T. Chu. On bounds for the normal integral. *Biometrika*, 42(1/2):pp. 263–265, 1955.
- [6] I. Daubechies, M. Defrise, and C. De Mol. An iterative thresholding algorithm for linear inverse problems with a sparsity constraint. *Communications on Pure and Applied Mathematics*, 57(11):1413–1457, 2004.
- [7] Zdzisław Denkowski, Stanisław Migórski, and Nikolas S. Papageorgiou. *An introduction to non-linear analysis: theory*. Kluwer Academic Publishers, Boston, MA, 2003.
- [8] David L. Donoho. For most large underdetermined systems of linear equations the minimal  $l_1$ -norm solution is also the sparsest solution. *Comm. Pure Appl. Math.*, 59(6):797–829, 2006.
- [9] Heinz W. Engl, Martin Hanke, and A. Neubauer. *Regularization of Inverse Problems*. Springer, 2000.
- [10] I. Loris, M. Bertero, C. De Mol, R. Zanella, and L. Zanni. Accelerating gradient projection methods for  $\ell_1$ -constrained signal recovery by steplength selection rules. *Applied and Computational Harmonic Analysis*, 27(2):247 – 254, 2009.
- [11] Hosein Mohimani, Massoud Babaie-Zadeh, and Christian Jutten. A fast approach for overcomplete sparse decomposition based on smoothed  $\ell^0$  norm. *IEEE Trans. Signal Process.*, 57(1):289–301, 2009.
- [12] Jorge Nocedal and Stephen Wright. *Numerical Optimization*. Springer, April 2000.
- [13] E. Polak and G. Ribière. Note sur la convergence de méthodes de directions conjuguées. *Rev. Française Informat. Recherche Opérationnelle*, 3(16):35–43, 1969.
- [14] B.T. Polyak. The conjugate gradient method in extremal problems. *{USSR} Computational Mathematics and Mathematical Physics*, 9(4):94 – 112, 1969.
- [15] J. R. Shewchuk. An Introduction to the Conjugate Gradient Method Without the Agonizing Pain. Technical report, Pittsburgh, PA, USA, 1994.

- [16] N. Z. Shor, Krzysztof C. Kiwiel, and Andrzej Ruszcayński. *Minimization Methods for Non-differentiable Functions*. Springer-Verlag New York, Inc., New York, NY, USA, 1985.
- [17] Vikas Sindhwani and Amol Ghoting. Large-scale distributed non-negative sparse coding and sparse dictionary learning. In *Proceedings of the 18th ACM SIGKDD International Conference on Knowledge Discovery and Data Mining*, KDD '12, pages 489–497, New York, NY, USA, 2012. ACM.
- [18] Albert Tarantola and Bernard Valette. Inverse Problems = Quest for Information. *Journal of Geophysics*, 50:159–170, 1982.